

GAMMA RAY BURST AND STAR FORMATION RATES: THE PHYSICAL ORIGIN FOR THE REDSHIFT EVOLUTION OF THEIR RATIO

MICHELE TRENTI^{1,†}, ROSALBA PERNA², SANDRO TACCHELLA³

Draft version January 8, 2022

ABSTRACT

Gamma Ray Bursts (GRBs) and galaxies at high redshift represent complementary probes of the star formation history of the Universe. In fact, both the GRB rate and the galaxy luminosity density are connected to the underlying star formation. Here, we combine a star formation model for the evolution of the galaxy luminosity function from $z = 0$ to $z = 10$ with a metallicity-dependent efficiency for GRB formation to simultaneously predict the comoving GRB rate. Our model sheds light on the physical origin of the empirical relation often assumed between GRB rate and luminosity density-derived star formation rate: $\dot{n}_{GRB}(z) = \varepsilon(z) \times \dot{\rho}_{obs}^*(z)$, with $\varepsilon(z) \propto (1+z)^{1.2}$. At $z \lesssim 4$, $\varepsilon(z)$ is dominated by the effects of metallicity evolution in the GRB efficiency. Our best-fitting model only requires a moderate preference for low-metallicity, that is a GRB rate per unit stellar mass about four times higher for $\log(Z/Z_{\odot}) < -3$ compared to $\log(Z/Z_{\odot}) > 0$. Models with total suppression of GRB formation at $\log(Z/Z_{\odot}) \gtrsim 0$ are disfavoured. At $z \gtrsim 4$, most of the star formation happens in low-metallicity hosts with nearly saturated efficiency of GRB production per unit stellar mass. However at the same epoch, galaxy surveys miss an increasing fraction of the predicted luminosity density because of flux limits, driving an accelerated evolution of $\varepsilon(z)$ compared to the empirical power-law fit from lower z . Our findings are consistent with the non-detections of GRB hosts in ultradeep imaging at $z > 5$, and point toward current galaxy surveys at $z > 8$ only observing the top 15 – 20% of the total luminosity density.

Subject headings: galaxies: high-redshift — galaxies: general — gamma-ray burst: general — stars: formation

1. INTRODUCTION

The star formation history of the Universe is a fundamental observable to understand the assembly and evolution of galaxies, the production of ionizing radiation and the gas chemical enrichment. Among the different (indirect) tracers of the star formation rate, two of particular relevance at high redshift are the measurement of the rest-frame UV luminosity density from galaxy surveys (e.g. Madau et al. 1998; Hopkins & Beacom 2006; Bouwens et al. 2011), and the rate of long-duration gamma-ray bursts (GRBs)(Kistler et al. 2009).

Deep surveys with ground and space telescopes identified thousands of galaxies up to redshift $z \lesssim 10$, when the Universe was just about 500 Myr old (Shimasaku et al. 2006; Bouwens et al. 2007, 2011; Ouchi et al. 2010; Trenti et al. 2011; Bradley et al. 2012; McLure, et al. 2013). However, converting luminosity density into a SFR depends upon stellar population properties, such as metallicity (Madau et al. 1998). In addition, dust obscuration is a severe problem for rest-frame U observations, especially at $z \lesssim 4$: The intrinsic luminosity density might be up to ten times larger than the observed one and is highly sensitive to dust correction estimates (Smit et al. 2012). Moreover, surveys are flux lim-

ited, hence the derived luminosity density traces the star formation rate (SFR) only in galaxies above detection threshold ($\dot{\rho}_{obs}^*(z)$). Because the galaxy luminosity function (LF) evolves with redshift, the amount of missed star formation changes as well, likely becoming more severe at high z , and is difficult to quantify directly (Trenti et al. 2010; Robertson et al. 2013).

Long-duration GRBs ($t > 2s$) are instead detectable at cosmological distances (Tanvir et al. 2009) and trace the SFR as well, since they are generally associated to the collapse of massive stars (MacFadyen & Woosley 1999). However, the number of events is much smaller compared to that of high- z galaxies, and more importantly there is likely a metallicity bias, related to a GRB production mechanism dependent on progenitor properties (Fruchter et al. 1999; Berger et al. 2003; Savaglio et al. 2009; Perley et al. 2013), for example because of reduced mass-loss rates in massive, low-metallicity stars (Yoon et al. 2006). The presence of such bias is supported by observations of a majority of low-metallicity hosts (e.g., Savaglio et al. 2009; Graham & Fruchter 2012; Jimenez & Piran 2013), although multiple cases of super-solar GRB hosts exist (Levesque et al. 2010; Savaglio et al. 2012; Perley et al. 2013). A further complication arises from understanding biases that dust obscuration (metallicity and redshift dependent) may introduce into the GRB rate ($\dot{n}_{GRB}(z)$) inference because of dark bursts (Perley et al. 2009; Greiner et al. 2011).

Given the complementary strenghts and weaknesses of both approaches, past investigations tried to connect them by typically assuming a relation:

$$\dot{n}_{GRB}(z) = \varepsilon(z) \times \dot{\rho}_{obs}^*(z), \quad (1)$$

trenti@ast.cam.ac.uk

¹ Institute of Astronomy and Kavli Institute for Cosmology, University of Cambridge, Madingley Road, Cambridge, CB3 0HA, United Kingdom

² JILA, Department of Astrophysical and Planetary Sciences, University of Colorado, 389-UCB, Boulder, CO 80309 USA

³ Department of Physics, Institute for Astronomy, ETH Zurich, CH-8093 Zurich, Switzerland

[†] Kavli Institute Fellow

where $\varepsilon(z)$ is the efficiency of GRB production per unit stellar mass, empirically assumed to have form:

$$\varepsilon(z) = \varepsilon_0(1+z)^\beta, \quad (2)$$

with $\beta \approx 1.2$ calibrated at $z \lesssim 4$ and then extrapolated at higher redshift (Kistler et al. 2009; Virgili et al. 2011; Robertson & Ellis 2012). The challenges with this empirical modeling are twofolds. First, the GRB rate depends physically on the *total* SFR ($\dot{\rho}_{tot}^*(z)$), not on $\dot{\rho}_{obs}^*(z)$ (derived from flux-limited galaxy surveys) as used in Equation 1, because the GRB afterglow is much brighter than its host and thus can be detected independently of host luminosity. Hence, one should have $\dot{n}_{GRB}(z) \propto \dot{\rho}_{tot}^*(z)$. Second, without a physical model to link GRB and star formation, there is no guarantee that Equation 2 holds beyond the redshift range of its calibration, raising concerns on systematic biases at $z \gtrsim 6$.

Here, we investigate the physical origin of the connection between GRB and SFR through $\varepsilon(z)$, and how this depends on metallicity of progenitors and on the difference between $\dot{\rho}_{tot}^*(z)$ and $\dot{\rho}_{obs}^*(z)$. We resort to a simple, yet successful model for the evolution of the galaxy UV LF (developed in Tacchella, Trenti & Carollo 2013; TTC13 hereafter), which we complement with the mass-metallicity relation for host galaxies from Maiolino et al. (2008) and with a metallicity-dependent GRB efficiency, inspired by stellar evolution simulations (Yoon et al. 2006). The setup of our modeling is described in Section 2, results in Section 3, conclusions in Section 4. As in TTC13, we adopt a WMAP5 cosmology: $\Omega_{\Lambda,0} = 0.72$, $\Omega_{m,0} = 0.28$, $\Omega_{b,0} = 0.0462$, $\sigma_8 = 0.817$, $n_s = 0.96$, $h = 0.7$ (Komatsu et al. 2009).

2. STAR FORMATION MODEL AND METAL-DEPENDENT GRB FORMATION

The base for our study is the model presented in TTC13, which links star formation to dark-matter halo assembly through a mass-dependent efficiency on a timescale defined by the halo assembly time, adopting a continuous star formation history over this timescale. Following Lacey & Cole (1993), this is the time needed to grow the main progenitor from halo mass $M_h/2$ to M_h . The key model feature is that the efficiency of star formation, $\xi(M_h) = M_*/M_h$, where M_* is the stellar mass, depends only on halo mass and is redshift independent (see also Behroozi et al. 2013). Since the halo assembly time is redshift dependent, the model naturally accounts for the redshift evolution of the rest-frame UV luminosity, computed using the Single Stellar Population models of Bruzual & Charlot (2003), at fixed halo mass (assembly times become shorter at high- z , thus halos are brighter). The model also includes treatment of dust extinction, which affects significantly the observed rest-frame UV luminosity of high- z galaxies, implemented with an empirically calibrated formula following Smit et al. (2012) (for comprehensive discussion see Sec. 3.3 in TTC13).

Given $\xi(M_h)$ and the DM halo mass function (from Sheth & Tormen 1999), the model thus fully describes the evolution of both the intrinsic galaxy LF, as well as that of the observed one (with dust extinction). All details on the efficiency of converting baryons into stars are encapsulated into $\xi(M_h)$. To calibrate this relation, we resort, like in TTC13, to abundance matching at

$z = 4$: Assuming that each DM halo hosts a single galaxy, we derive $\xi(M_h)$ so that the model, dust-extinct, LF has a Schechter form ($\phi(L) = \phi^*(L/L^*)^\alpha \exp(-L/L^*)$) with parameters: $\phi^* = 1.3 \times 10^{-3} \text{ Mpc}^{-3}$; $\alpha = -1.73$ and $M_{AB}^* = -21.0$, where $M^* = -2.5 \log_{10} L^*$ (Bouwens et al. 2007). Note that TTC13 account for scatter in the luminosity to halo-mass relation, and for a burst of star formation at the halo assembly time as additional free-parameter to calibrate. Both features only add modest improvements on the data-model comparison for the LF and star formation rates, so we neglect them here. Our simplified model is still capable of an overall good description of the star formation rate evolution over the whole history of the Universe (Fig. 1, left panel), and allows us to explore the link to the production of GRB events while minimizing the free parameters.

Compared to other recent investigations on the connection between GRB production and SFR (Robertson & Ellis 2012; Hao & Yuan 2013), our framework has the advantage of relying on a physical model for the galaxy LF, therefore allowing us to explore the effects of star formation below the observational limit of the deepest galaxies survey. This way, we can address what is the contribution to the GRB production by dwarf-like galaxies at high- z which are too faint for direct observations, with high complementarity to the recent modeling by Jimenez & Piran (2013) at $z \lesssim 3$ by means of reconstruction of the star formation history from SDSS observations of local galaxies.

In addition, to investigate whether and how much GRB production is preferentially located in low-metallicity environments, we augment our model using the mass-metallicity relation of Maiolino et al. (2008) to assign galaxy metallicities. For this, we adopt their Equation 2 with coefficients from Table 5 (for Bruzual & Charlot 2003 models) and linear interpolation in redshift space. Then, we resort to stellar evolution simulations by Yoon et al. (2006) to construct a basic form for the metallicity-dependent efficiency of GRB formation. The main limitation is that, because simulations of GRB progenitors are computationally expensive, Yoon et al. (2006) only explore a limited number of models, with coarse sampling of metallicity (see their Figs. 3 and 6). Broadly, they conclude that very low metallicity progenitors ($Z \lesssim 10^{-3} Z_\odot$) are two-three times more likely to produce GRBs compared to low metallicity ones ($Z \sim 10^{-1} Z_\odot$), and that efficiency drops to ~ 0 for higher content of metals. The latter conclusion is however in tension with recent observations of GRB hosts with $Z \sim Z_\odot$ (Levesque et al. 2010; Elliott et al. 2013), and might be related to the limited parameter space explored by the Yoon et al. (2006) simulations. Alternatively, channels for GRB production which are different from the Collapsar model and do not require low metallicity progenitors have been proposed, such as binary systems (Fryer & Heger 2005; Podsiadlowski et al. 2010). Therefore, we include in our metallicity-dependent efficiency a plateau of non-zero probability of forming GRBs which is metallicity-independent, treating this as a free parameter to explore by comparison with the observed GRB rate. The piece-wise linear functional form for our metal-

dependent efficiency of GRB production is:

$$\kappa(Z) = \kappa_0 \times \frac{a \log_{10} Z/Z_\odot + b + p}{1 + p}, \quad (3)$$

where κ_0 and p are free parameters (normalization of the relation and efficiency plateau at $Z \geq Z_\odot$), while a and b depend on Z as follows. For $Z/Z_\odot \leq 10^{-3}$, $a = 0$, $b = 1$; for $10^{-3} \leq Z/Z_\odot \leq 10^{-1}$, $a = -3/8$, $b = -1/8$; for $10^{-1} \leq Z/Z_\odot \leq 1$, $a = -1/4$, $b = 0$; for $Z/Z_\odot > 1$, $a = 0$, $b = 0$. Fig. 4 shows $\kappa(Z)$ for $\kappa_0 = 1$ and $p = 0.3$ (our fiducial plateau value).

For a model with given threshold in minimum halo mass for star formation and given efficiency of forming GRBs in high-metallicity environments (parameter p), we determine κ_0 (normalization of GRB efficiency production) by carrying out a least-square fit of our predicted GRB rate by comparison with Wanderman & Piran (2010) (Fig. 1, right panel). We limit the fit to points at $z \leq 6$ because of growing uncertainty in observations at higher redshift.

3. MODELING RESULT

Our canonical model assumes that star formation proceeds down to halos with mass $M_h \geq 10^8 M_\odot$, approximately equivalent to virial temperatures $T_{vir} \gtrsim 10^4$ K, sufficient for cooling and forming stars even in presence of a UV background, albeit at very low efficiency (Trenti et al. 2009; Finlator et al. 2011). We predict that these halos host very faint galaxies with magnitude $-12 \lesssim M_{UV} \lesssim -10$, depending on redshift.⁵ For the efficiency of GRB production with metallicity, we assume $p = 0.3$ in Equation 3, so that we form a (small) fraction of GRBs in high-metallicity environments. The results of the comparison of the model predictions to the data are shown in Fig. 1. The model (black-dashed line) captures well the evolution of the observed SFR $\dot{\rho}_{obs}^*(z)$ (data points from a variety of surveys, see Fig. 2 in TTC13 for full details), derived from the luminosity density for galaxies with $M_{AB} \leq -17.7$. At $z \lesssim 3$, integrating over the model LF to $M_{AB} \leq -11$ (thus including faint galaxies), yields an approximately constant increase of the SFR by a factor ~ 1.3 (red-solid line). At higher redshift there is a growing fraction of star formation in small mass, low luminosity halos, so that at $z \gtrsim 8$ only $\lesssim 20\%$ of all star formation is seen in current surveys (see also Trenti et al. 2010 for similar conclusions). The model prediction for the GRB rate, which derives from the SFR for all galaxies, weighted by the metallicity preference for low- Z hosts, is shown as red-solid line in the right panel of Fig. 1 and describes the data well.

In Fig. 2 we use these results to investigate our predictions for the relation $\varepsilon(z)$ between the SFR and GRB rate (Equation 1), empirically modeled as power law in redshift by past studies (Equation 2). Our model (red-solid line) predicts indeed an approximate power law with $\beta = 1.2$, as derived by Virgili et al. (2011); Robertson & Ellis (2012), in the redshift range where the large majority of GRBs are observed ($1 \lesssim z \lesssim 5$).

⁵ For comparison, the deepest observations in the HUDF field reach $M_{UV} \sim -17$ (Bouwens et al. 2007), but recently Alavi et al. (2013) used gravitational lensing to probe the $z \sim 2$ UV LF down to $M_{UV} \sim -13$, demonstrating that it remains a steep power law, like in our model.

We predict deviations from a power law both in the local Universe and at very high z , with our model staying above $(1+z)^{1.2}$. To understand the physical origin of $\varepsilon(z)$, we decompose the contribution to this quantity in metallicity effect (green-dashed line) and faint galaxies (blue-dashed line). We see immediately that metallicity evolution is the main driver of $\varepsilon(z)$ at $z \lesssim 5$. At higher z , though, most of the star formation happens in low-luminosity, small mass galaxies, where the mass-metallicity relation predicts low Z and near-maximal GRB production per unit stellar mass. Therefore, based on metallicity alone one would predict a flattening of $\varepsilon(z)$ at high z . However, around the same redshift at which the metal-dependent efficiency of GRB production saturates, the fraction of missed star formation in faint galaxies begins to increase steadily. This is the driver of the accelerated growth of $\varepsilon(z)$ at $z \gtrsim 5$. Finally, we note that at low redshift our model predicts a slight excess of GRBs compared to the observed GRB rate (Fig. 1) and to $\varepsilon(z) \sim (1+z)^\beta$. While we stress that there is no physical reason because $\varepsilon(z)$ should be a power law, it is nevertheless possible that a more accurate parameterization of $\kappa(Z)$ would give better agreement.

Overall, our canonical model provides a comprehensive description of the data both for $\dot{\rho}_{obs}^*(z)$ and for $\dot{n}_{GRB}(z)$. To further understand how unique/robust these predictions are, it is useful to compare them to those obtained by varying model parameters. This is illustrated for $\dot{n}_{GRB}(z)$ in Fig. 3, for a range of different assumptions that all give by construction the same description of the observed SFR $\dot{\rho}_{obs}^*(z)$. Fig. 3, left panel, explores the effects of varying the metallicity-dependence in GRB production. The blue line shows predictions for complete suppression of GRBs in high metallicity progenitors ($p = 0$), while the green line has no metallicity dependence ($p \rightarrow +\infty$). It is immediate to see that both scenarios represent a worse description of the data ($\chi^2 = 9.5$ and $\chi^2 = 5.6$ respectively) compared to the canonical model (red, $\chi^2 = 2.1$), with systematic deviations which introduce autocorrelation in the residuals at low and high redshift (going into opposite directions). The right panel illustrates the same three models, but here we assume that there is no star formation in galaxies with $M_{AB} > -17.7$ (this means $\dot{\rho}_{obs}^*(z) \equiv \dot{\rho}_{total}^*(z)$). Scenarios with both extreme and no metallicity dependence are similarly disfavored ($\chi^2 = 383$ and $\chi^2 = 6.9$ respectively). Interestingly the current data from $\dot{n}_{GRB}(z)$ alone don't rule out that GRBs originate from star formation sites with $M_{AB} \lesssim -17.7$ ($\chi^2 = 1.9$). In fact, at $z \lesssim 5$ the models with and without faint galaxies are essentially yielding the same predictions, just with a different κ_0 normalization. However, as we discussed in Trenti et al. (2012), searches for host-galaxies of GRBs at high- z are a powerful probe to investigate whether star formation is happening in low-luminosity galaxies. From the non-detection of $n = 6$ GRB host galaxies at $z > 5$, we can confidently exclude this alternative scenario (Trenti et al. 2012; see also Tanvir et al. 2012). We thus conclude that by combining all available observations, the best model is the one predicting a growing abundance of faint galaxies as the redshift increases, along with a moderate preference for GRBs to form in low-metallicity environments ($p \approx 0.3$). Without dupli-

cating the discussion of Trenti et al. (2010, 2012), this strengthens the conclusion that the majority of the ionizing photons at $z > 6$ are produced by galaxies currently too faint to be observed in ultradeep fields with the Hubble Space Telescope (see also Shull et al. 2012).

4. CONCLUSIONS

In this *letter* we investigated the relation between star formation and GRB rate. For this, we resorted to a physical model which describes the galaxy LF evolution from $z = 0$ to $z = 10$, augmented it with a mass-metallicity relation, and assumed a metallicity-dependent efficiency for GRB production. We showed that we can construct a successful GRB-rate model assuming that star formation continues down to galaxies with $M_{AB} \lesssim -11$ and that GRBs are about four times more likely to originate in very low metallicity environments ($Z/Z_{\odot} < 10^{-3}$) compared to $Z \sim Z_{\odot}$. With this model we investigated the physical origin for the redshift evolution of the ratio between GRB and SFR ($\varepsilon(z)$, Equation 2). We showed that the approximate $(1+z)^{1.2}$ behavior empirically derived by previous studies at $z \lesssim 4$ is driven primarily by metallicity dependence. Importantly, our model predicts a steepening of such relation at higher z , because of a growing fraction of star formation happening in galaxies with $M_{AB} > -17.7$ during the epoch of reionization at $z \gtrsim 5$.

Our model can be used to derive an improved estimate of the total SFR at $z > 4$ from GRB events, compared to past investigations which rely on extrapolation of $\varepsilon(z) \propto (1+z)^{\beta}$ beyond $z > 4$ (Fig. 1). In this respect, we note that we are obtaining a self-consistent description of both SFR and GRB rate, as well as of the stellar mass density with redshift (the latter is discussed in TTC13, e.g. see their Fig. 2). In contrast, Robertson & Ellis (2012) argue that the GRB-inferred star formation rate is inconsistent with the stellar mass assembly. Their result is likely due to the extrapolation for $\varepsilon(z)$, which leads to an overestimate of the SFR inferred from GRBs (since their $\varepsilon(z)$ is underestimated at $z > 4$ based on our conclusions). Overall, we can

conclude that there is no tension between using either the GRB rate or the observed luminosity density from galaxy surveys as tracers of star formation, provided that the presence of faint galaxies below the current detection limits is taken into account.

Of course, the uncertainties on the data, especially on the GRB rate, are still large. Thus, it is fundamental to identify additional independent tests of the framework we introduced. For example, Jimenez & Piran (2013) assume that GRB production has a hard cut-off at $Z/Z_{\odot} \geq 0.1$ and obtain a good match to $\dot{n}_{GRB}(z \lesssim 3)$ considering the star formation history at $z \lesssim 3$ reconstructed from stellar archeology observations of galaxies in the local Universe. At higher redshift ($z \gtrsim 3$), some GRBs might have Population III progenitors forming in rare pockets of metal free gas, predicted theoretically (Trenti et al. 2009), and recently observed (Fumagalli et al. 2011). To better discriminate among all these different models, a promising approach would be to use our model to construct predictions for how the LF of GRB hosts at $z \sim 1-3$ differs from the one observed for Lyman-break galaxies. With a growing sample of GRB hosts being identified by nearly-complete follow-up surveys such as TOUGH (Hjorth et al. 2012) such comparison should be achievable in the near future. This will provide validation/refinement for our current treatment of the metallicity bias. In addition, ultradeep follow-up observations of host galaxies of GRBs at $z \gtrsim 5$ have the potential to quantify the fraction of missed star formation in galaxy surveys such as the Hubble Ultradeep Field (Bouwens et al. 2011), providing a highly complementary tool to investigate star formation during the epoch of reionization without waiting for next generation facilities such as the *James Webb Space Telescope*.

We thank Raul Jimenez, Roberto Maiolino, Max Pettini, and Sandra Savaglio for useful discussions. This work was partially supported by the European Commission through the Marie Curie Career Integration Fellowship PCIG12-GA-2012-333749 (MT) and by NSF Grant No. AST 1009396 (RP).

REFERENCES

- Alavi, A., Siana, B., Richard, J. et al. 2013, ApJ, submitted, arXiv:1305.2413
- Behroozi, P. S., Wechsler, R. H., & Conroy, C. 2013, ApJ, 762, 31
- Berger, E., Cowie, L. L., Kulkarni, S. R., et al. 2003, ApJ, 588, 99
- Bouwens, R. J., Illingworth, G. D., Franx, M. & Ford, H. 2007, ApJ, 670, 928
- Bouwens, R. J., Illingworth, G. D., Oesch, P. A. et al. 2011, ApJ, 737, 90
- Bradley, L. D., Trenti, M., Oesch, P. A., et al. 2012, ApJ, 760, 108
- Bruzual, G., & Charlot, S. 2003, MNRAS, 344, 1000-1028
- Elliott, J., Krühler, T., Greiner, J. et al. 2013, A&A, submitted, arXiv:1306.0892
- Fruchter, A. S. Thorsett, S. E., Metzger, M. R. et al. 1999, ApJ, 519, 13
- Finlator, K., Oppenheimer, B. D. & Davé, R. 2011, MNRAS, 410, 1703
- Fryer, C. L. & Heger, A. 2005, ApJ, 623, 302
- Fumagalli, M., O’Meara, J. M. & Prochaska, J. X. 2011, Science, 334, 1245
- Graham, J. F. & Fruchter, A. S. 2012, arXiv:1211.7068
- Greiner, J., Krühler, T., Klose, S. et al. 2011, A&A, 526, A30
- Hao, J. & Yuan, Y. 2013, ApJ, accepted, arXiv:1305.5165
- Hjorth, J., Malesani, D., Jakobsson, P., et al. 2012, ApJ, 756, 187
- Hopkins, A. M. & Beacom, J. E., ApJ, 651, 142
- Kistler, M. D., Yüksel, H., Beacom, J. F. et al. 2009, ApJ, 705, L104
- Komatsu, E., Dunkley, J., Nolta, M. R., et al. 2009, MNRAS, 180, 330-376
- Lacey, C., & Cole, S. 1993, MNRAS, 262, 627-649
- Levesque, E. M., Soderberg, A. M., Kewley, L. J. & Berger, E. 2010, ApJ, 725, 1337
- Jimenez, R. & Piran, T. 2013, ApJ, accepted, arXiv:1303.4809
- Madau, P., Pozzetti, L., & Dickinson, M. 1998, ApJ, 498, 106
- Maiolino, R., Nagao, T., Grazian, A. et al. 2008, A&A, 488, 463
- MacFadyen, A. I. & Woosley, S. E. 1999, ApJ, 524, 262
- McLure, R. J., Dunlop, J. S., Bowler, R. A. A., et al. 2013, MNRAS, in press, arXiv:1212.5222
- Ouchi, M., Shimasaku, K., Furusawa, H., et al. 2010, ApJ, 723, 869
- Perley, D. A., Cenko, S. B., Bloom, J. S. et al. 2009, AJ, 138, 1690
- Perley, D. A., Levan, A. J., Tanvir, N. R. et al. 2013, ApJ, submitted, arXiv:1301.5903
- Podsiadlowski, P., Ivanova, N., Justman, S. & Rappaport, S., 2010, MNRAS, 406, 840
- Robertson, B. E. & Ellis, R. S. 2012, ApJ, 744, 95
- Robertson, B. E., Furlanetto, S. R., Schneider, E. et al., 2013, ApJ, 768, 71
- Savaglio, S., Glazebrook, K. & Le Borgne, D. 2009, ApJ, 691, 182
- Savaglio, S., Rau, A., Greiner, J. et al. 2012, MNRAS, 420, 627
- Schechter, P. 1976, ApJ, 203, 297
- Sheth, R. K., & Tormen, G. 1999, MNRAS, 308, 119-126
- Shimasaku, K., Kashikawa, N., Doi, M., et al. 2006, PASJ, 58, 313

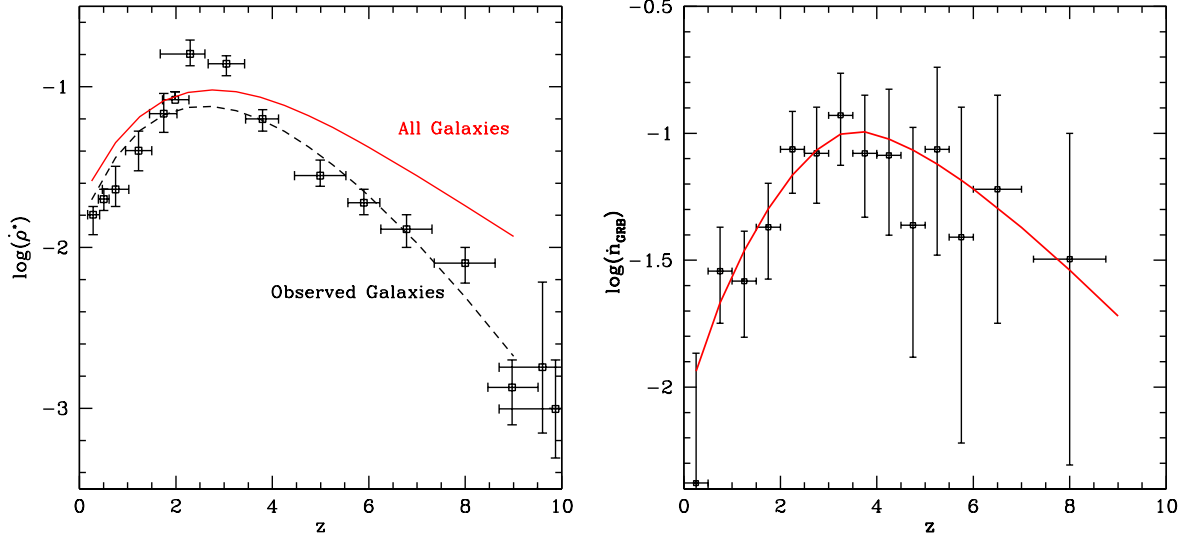


FIG. 1.— Left panel: Star formation rate versus redshift, inferred from LBG observations in the UV integrated to $M_{AB} = -17.7$ and corrected for dust extinction (see TTC13). The black-dashed line shows predictions from our LF model integrated to the same observational limit. The red-solid line shows instead the model with LF integrated over all galaxies ($M_{AB} \lesssim -11$). Right panel: GRB comoving rate from Wanderman & Piran (2010) compared to predictions of our best fitting model, which includes a moderate metallicity-dependence on the GRB rate (see Fig. 4).

Shull, J. M., Harness, A., Trenti, M. & Smith, B. D. 2012, ApJ, 747, 100
 Svensson, K. M., Levan, A. J., Tanvir, N. R., et al. 2010, MNRAS, 505, 47
 Smit, R., Bouwens, R. J., Franx, M., et al. 2012, ApJ, 756, 14
 Tanvir, N. R., Fox, D. B., Levan, A. J. et al. 2009, Nature, 461, 1254
 Tanvir, N. R., Levan, A. J., Fruchter, A. S. et al. 2012, ApJ, 754, 46
 Trenti, M., Stiavelli, M. & Shull, J. M. 2009, ApJ, 700, 1672
 Trenti, M., Stiavelli, M., Bouwens, R. J. et al. 2010, ApJ, 714, L202

Trenti, M., Bradley, L. D., Stiavelli, M. et al. 2011, ApJ, 727, L39
 Trenti, M., Perna, R., Levesque, E. M. et al. 2012, ApJL, 749, 38
 Tacchella, S., Trenti, M. & Carollo, C. M. 2013, ApJ, 768, 37 [TCC13]
 Virgili, F. J., Zhang, B., Nagamine, K. & Choi, J. 2011, MNRAS, 417, 3025
 Wanderman, D. and Piran, T. 2010, MNRAS, 406, 1944
 Yoon, S. C., Langer, N. & Norman, C. 2006, A&A, 460, 199

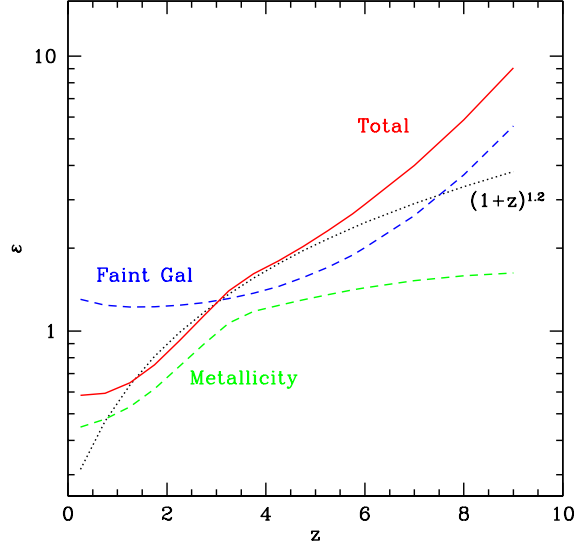


FIG. 2.— Redshift evolution of the GRB rate to SFR ratio $\varepsilon(z)$ (red-solid line). Our model highlights that at low redshift the metallicity evolution is the main driver of $\varepsilon(z)$ (green-dashed line), while at high- z changes in $\varepsilon(z)$ are primarily due to an increasing fraction of integrated light missed in flux-limited LBG surveys (blue-dashed line). At $z > 5$ we see an accelerated evolution of $\varepsilon(z)$ compared to the best fitting power-law $(1+z)^{1.2}$ derived at $z \lesssim 5$ (black-dotted line).

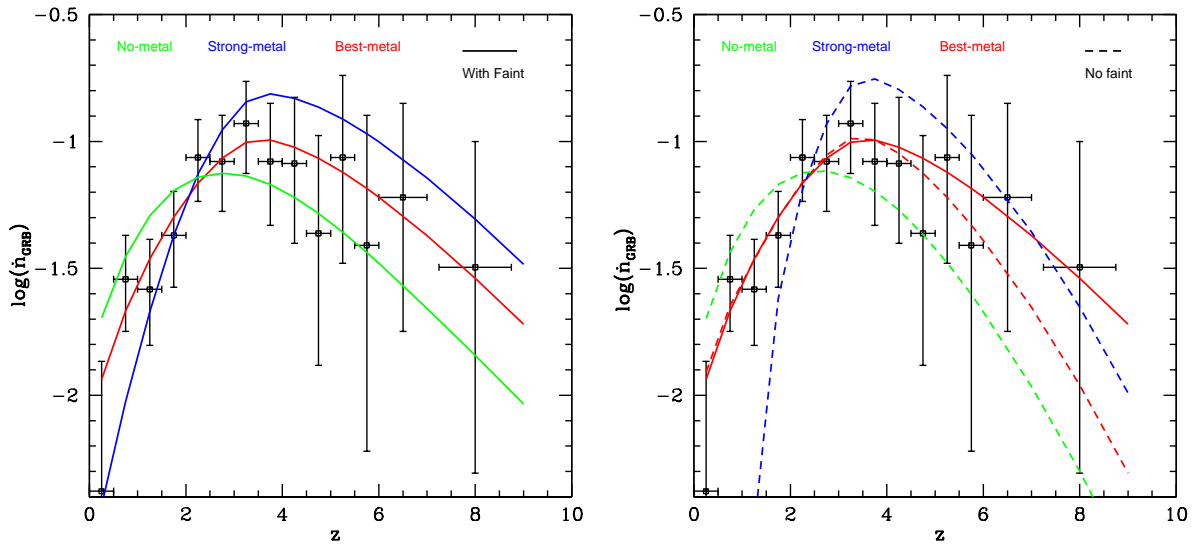


FIG. 3.— Left panel: GRB comoving rate for models with different efficiencies for forming GRBs as function of metallicity, compared to the Wanderman & Piran (2010) rate. The red solid line is our reference model; the blue line represents a model with complete suppression of GRB formation in $Z > Z_{\odot}$ environments, and the green line is a model without metallicity dependence ($\kappa(Z)$ constant). Right panel: same as left panel but for models where star formation happens only in galaxies with $M_{AB} \leq -17.7$. A model with moderate metallicity dependence still provides an acceptable fit without assuming star formation below the observational limit (red-dashed line). Such model is however in strong tension (ruled out at $> 99\%$ confidence) with the non-detection of GRB host galaxies at $z > 5$ (see Trenti et al. 2012; Tanvir et al. 2012).

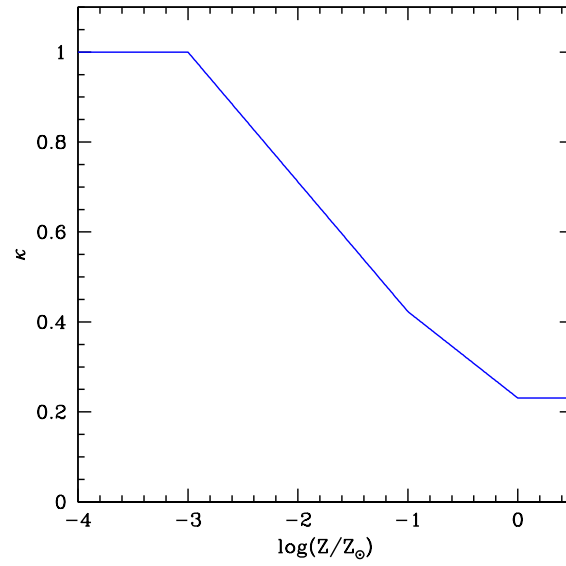


FIG. 4.— Functional form for efficiency of GRB production per unit stellar mass versus host-galaxy metallicity for our fiducial model. GRBs are about four times more likely in low metallicity progenitors compared to super-solar ones.